Available online at www.sciencedirect.com
ScienceDirect
Physica A 387 (2008) 1446–1454
PHYSICA A
www.elsevier.com/locate/physa

Stochastic resonance of a periodically driven neuron under non-Gaussian noise

J.R.R. Duarte, M.V.D. Vermelho, M.L. Lyra*

Instituto de Física, Universidade Federal de Alagoas, 57072-970 Maceió - AL, Brazil

Received 29 August 2007; received in revised form 25 October 2007
Available online 13 November 2007

Abstract

We investigate the first-passage-time statistics of the integrate–fire neuron model driven by a sub-threshold harmonic signal superposed with a non-Gaussian noise. Here, we considered the noise as the result of a random multiplicative process displaced from the origin by an additive term. Such a mechanism generates a power-law distributed noise whose characteristic decay exponent can be finely tuned. We performed numerical simulations to analyze the influence of the noise non-Gaussian character on the stochastic resonance condition. We found that when the noise deviates from Gaussian statistics, the resonance condition occurs at weaker noise intensities, achieving a minimum at a finite value of the distribution function decay exponent. We discuss the possible relevance of this feature to the efficiency of the firing dynamics of biological neurons, as the present result indicates that neurons would require a lower noise level to detect a sub-threshold signal when its statistics departs from Gaussian.
© 2007 Elsevier B.V. All rights reserved.

PACS: 05.40.-a; 02.50.Ey; 87.19.La

Keywords: Stochastic resonance; Non-Gaussian noise; Integrate–fire model

1. Introduction

The idea of stochastic resonance has been widely applied in investigating many physical, chemical and biological systems, including optical, electronic and magnetic systems [1], chemical reactions [2] and neuro-physiological aspects of sensory systems [3–5]. It has been extensively investigated in dynamical models of periodically stimulated sensory neurons [1,6–8]. In the basic integrate–fire neuron model the state of the neuron is described in terms of its membrane potential resulting from synaptic inputs. When the membrane potential reaches a threshold, a spike is generated indicating an action potential. The spike train exhibits a statistical phase lock to the sub-threshold stimulus added to noise. The distribution of the interspike intervals, like the first-passage-time distribution, presents regular peaks signaling the sub-threshold signal. The intensity of these peaks goes through a maximum as the noise intensity is increased.

Analytical and numerical studies of stochastic resonance usually consider the noise to be uncorrelated in time (white) and Gaussian, a good approximation to model systems where the relaxation time of the noise auto-correlation

* Corresponding author.
E-mail address: marcelo@fis.ufal.br (M.L. Lyra).

0378-4371/$ - see front matter © 2007 Elsevier B.V. All rights reserved.
doi:10.1016/j.physa.2007.11.011

is much shorter than the characteristic time scale of the dynamical system. The effect of the noise correlation time in a bistable system was first investigated by Gammaitoni et al. [9] showing a degradation of the resonance effect due to the competition between the noise correlation time and the average time of waiting between noise-induced inter-well transitions. Correlations also play a relevant role in the stochastic resonance of neuron models [10–13]. An experimental study of the effect of correlated (colored) noise in the stochastic resonance of sensory neurons showed that, for low frequencies of the periodic signal, conventional white noise presents the lowest optimal noise intensity and the highest signal-to-noise ratio as compared with colored noise [14]. However, the same study suggested that colored $1/f$ noise may be better than white noise at high frequencies, providing a possible explanation for the wide occurrence of $1/f$ noise in biological systems, a feature reinforced by more recent works [15,16].

Stochastic resonance induced by colored and non-Gaussian noises has also been recently investigated [17–21] showing an enhancement on the signal-to-noise ratio when the noise departs from Gaussian behavior. Also, a numerical investigation of stochastic resonance in bistable systems driven by a white noise with power-law distributed intensities showed that an optimal transition rate can be achieved for a finite decay exponent of the noise probability distribution [22]. There is a growing interest in studying dynamical systems driven by non-Gaussian noises with slowly decaying power-law distribution, given that they are quite ubiquitous in natural phenomena [23]. One of the simplest mechanisms for generating a power-law distributed noise is through a random multiplicative process (RMP) [24–26]. This mechanism has been widely used to model stochastic series emerging, for example, in economics [27–29] and biology [30–32]. It has been shown that, when the multiplicative random process acts together with an additive noise term, or more generally when the dynamical variable is repelled from the origin, true power-law distributed random series can be generated [24,25].

In this work, we will study the dynamics of the integrate and fire model for the neural response driven by a periodic sub-threshold signal and under the influence of a non-Gaussian noise generated by a random multiplicative process. We will be particularly interested in evaluating the first-passage-time distribution whose peaks may reveal the main time scale of the underlying periodic signal. The intensity of these peaks passes through a maximum when varying the noise intensity, a typical signature of stochastic resonance. We will give a detailed analysis of the resonance condition as a function of the noise statistics to show that optimal efficiency in recognizing the sub-threshold signal can be achieved at weaker noises when its statistics departs from the Gaussian behavior.

2. Model and numerical procedure

The integrate–fire neuron model has been widely used as the standard model for investigating the dynamics of neural systems. It is able to qualitatively describe the sub-threshold integration which occurs on a time scale much slower than that involved in the spike generation. Within this approach, the membrane potential of a periodically driven neuron is assumed to obey the stochastic differential equation

$$\frac{\mathrm{d}x}{\mathrm{d}t} = -\gamma x + \mu + A\sin(\omega t + \phi) + v(t), \tag{1}$$

where γ is the inverse of the membrane time constant and μ/γ is the equilibrium membrane potential in the absence of external inputs. $v(t)$ represents a source of noise for the synaptic inputs which superposes with the periodic stimulus. The above stochastic equation is to be complemented with a spike-and-reset rule. Whenever the membrane voltage x reaches a threshold value Θ, a spike is generated and the membrane potential is reset to $x = 0$.

In order to investigate the stochastic resonance, the amplitude of the periodic input should be weak, so that the oscillations that it induces in the membrane voltage are not enough to promote the threshold crossing. The threshold crossing and the consequent neuron spike are ultimately due to the presence of noise. In what follows, we will be particularly interested in the statistics of the first-passage time. This quantity can be obtained analytically from simplified approaches [34–37], thus allowing a direct verification of numerical results. Other relevant quantities are related to the spike sequence and the interspike-interval distribution. For an endogenous periodic input, which is reset to its initial phase after each spike (taken to be $\phi = 0$), these two distributions coincide. Endogenous stimuli are biologically unrealistic and some features are artifacts of such reduced dynamics [38]. For exogenous stimuli, the statistics of the first-passage time and the interspike intervals are distinct, especially when neuron spikes are induced at weak noise. However, noise-induced phenomena found in the interspike-interval distribution show comparable resonance effects with and without the stimulus reset [34,39,40]. The average interval between spikes, like the average

first-passage time, decreases with increasing noise amplitude. For intermediate noises, there is a statistical phase locking to the underlying sub-threshold periodic signal that gives the optimal signature of its characteristic time scale. Usually, the noise input is considered to be Gaussian and delta correlated (white). Here, the noise will be taken as resulting from a random multiplicative process, which can be described by the following stochastic differential equation:

$$\frac{\mathrm{d}v}{\mathrm{d}t} = \lambda(t)v(t) + \eta(t), \tag{2}$$

where $\lambda(t)$ is a multiplicative noise and $\eta(t)$ an additive noise. Both $\lambda(t)$ and $\eta(t)$ are white and Gaussian, with average and variance given by

$$\langle\lambda(t)\rangle = \lambda < 0, \quad \langle(\lambda(t) - \lambda)(\lambda(t') - \lambda)\rangle = 2D_\lambda\delta(t - t'), \tag{3}$$

and

$$\langle\eta(t)\rangle = 0, \quad \langle\eta(t)\eta(t')\rangle = 2D_\eta\delta(t - t'). \tag{4}$$

In what follows, the additive noise will be assumed to be much weaker than the multiplicative noise. The Fokker–Planck equation satisfied by the probability distribution function $P(v, t)$ of $v(t)$ can be shown to be given by

$$\frac{\partial}{\partial t}P = -\frac{\partial}{\partial v}\left[(\lambda + D_\lambda)vP - \frac{\partial}{\partial v}[(D_\lambda v^2 + D_\eta)P]\right], \tag{5}$$

which has as stationary solution

$$P(v) \propto \left[1 + \left(\frac{v}{s}\right)^2\right]^{-(\beta+1)/2}, \tag{6}$$

with $s = \sqrt{D_\eta/D_\lambda}$ and $\beta = -\lambda/D_\lambda$. Boundary conditions with no probability flux were assumed to produce stationarity (see e.g. Ref. [33] for details concerning the stochastic prescription leading to Eq. (5)). The strength of the noise generated can be characterized by its variance $2D_v = \langle v^2\rangle = D_\eta/[D_\lambda(\alpha - 3/2)]$. The weak additive noise condition implies $s \ll 1$ with the stochastic signal having an asymptotic power-law distribution $P(v/s \gg 1) \propto (v/s)^{-2\alpha}$. The characteristic power-law exponent $2\alpha = \beta + 1$ is, therefore, determined only by statistical characteristics of the multiplicative noise.

In the following section, we will investigate the sensitivity of the stochastic resonance condition of the driven integrate–fire neuron model to the statistical distribution of the input noise. The average multiplicative noise λ will be used to tune the power-law distribution exponent. Without loss of generality, we will use units of $D_\lambda = 1$. The variance of the input noise $v(t)$ will then be varied through control of the additive noise variance.

3. First-passage-time distribution

We solved the integrate–fire and multiplicative noise differential equations by using numerical algorithms which were devised to deal with stochastic differential equations involving both additive and multiplicative noises [41]. The discretization of Eq. (2) was written in the form

$$\mathrm{d}v(t) = \lambda v(t)\mathrm{d}t + \mathrm{d}W_\lambda + \frac{1}{2}v(t)(\mathrm{d}W_\lambda)^2 + \mathrm{d}W_\eta, \tag{7}$$

where $\mathrm{d}W_x$ ($x = \lambda, \eta$) represents the Wiener process increment resulting from the integration of the noise x over the time interval $\mathrm{d}t$. According to the central limit theorem, $\mathrm{d}W_x$ has a Gaussian distribution with variance $2D_x\mathrm{d}t$. Therefore, during the numerical integration, the Wiener increments were simulated by $\mathrm{d}W_x = R_G\sqrt{2D_x\mathrm{d}t}$, where R_G was taken as a random number sampled from a Gaussian distribution with unitary variance. For the multiplicative noise, the quadratic term in the Wiener increment was included to improve the convergence, according to Ito's prescription. It effectively takes as a better approximation of $v(t)$ its average value at the beginning and end of the integration interval $\mathrm{d}t$.

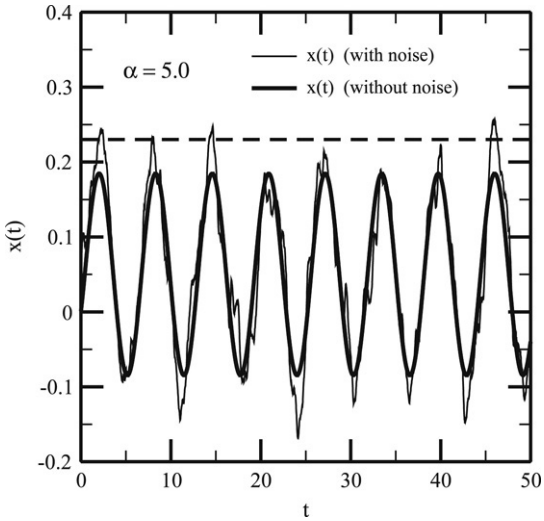

Fig. 1. The time evolution of the membrane potential. The solid thick line corresponds to the periodic oscillations of the membrane potential driven by a pure harmonic input. The solid thin line is the membrane potential for superposed harmonic and noise signals. The potential reset after the threshold crossing was not performed, to better illustrate the statistical phase locking of the crossings with the underlying sub-threshold signal. Here, the parameters used were $\gamma = 2$, $A = 0.3$, $\mu = 0.1$, $\omega = 1$, $D_\eta = 1.5 \times 10^{-3}$, $\lambda = -9$ ($\alpha = (\beta + 1)/2 = 5$). The threshold level $\Theta = 0.23$ (represented here as a dashed line) was considered in the analysis of the first-passage-time distribution.

The following results were obtained by using as a representative set of dimensionless parameters $\gamma = 2$, $A = 0.3$, $\omega = 1$, $\mu = 0.1$, $\Theta = 0.23$ and a discretization time $\mathrm{d}t = 0.01$. However, the following results are not affected qualitatively by this particular choice of parameters. The time scale can be adjusted to experimental data by comparing $1/\gamma$ with the membrane time constant. Potentials are in units of $D_\lambda = 1$. For this set of parameters, the equilibrium membrane potential is $x_0 = 0.05$. The periodically driven system in the absence of noise develops sub-threshold oscillations, with the maximum of the membrane potential reaching approximately $x_{max} = x_0 + A/\sqrt{\gamma^2 + \omega^2} = 0.184 < \Theta$. As the noise resulting from the random multiplicative process is added to the periodic input signal, the membrane potential develops periodically modulated fluctuations and noise-induced threshold crossings. In Fig. 1 we display a typical plot of the time evolution of the membrane potential in which the potential reset rule due to neuron firing after the threshold crossing is not applied.

The proper integration of the stochastic differential equation with both multiplicative and additive noise is a key aspect of the following analysis of the influence of the non-Gaussian character of the noise on the stochastic resonance condition of the integrate–fire neuron model. In Fig. 2 we depict two random series generated from the numerical solution of Eq. (2), with $\alpha = 5.0$ and $\alpha = 1.5$ (bottom panel). According to Eq. (6), the first one will have an almost Gaussian distribution while the second one has a strong non-Gaussian distribution with a slowly decaying tail. The presence of spikes in the second series already anticipates that large events occur at a much larger frequency than expected for a Gaussian random process. In Fig. 3 we report the measured probability distribution function of these series, which are in perfect agreement with Eq. (6).

The enhanced probability of occurrence of large events, which is favored as the noise probability distribution deviates further from Gaussian behavior, is expected to reduce the average first-passage time even when the noise level is kept fixed. In Fig. 4 we report the measured first-passage-time distribution as obtained for a fixed variance of the additive noise $D_\eta = 3.10 \times 10^{-3}$ and two distinct non-Gaussian neuron input noises with $\alpha = 5$ (slightly non-Gaussian) and $\alpha = 1.5$ (strongly non-Gaussian). The intervals between the peaks reveal the period of the sub-threshold harmonic signal. Their positions are closely located at the maxima of the harmonic signal $t_n = 2\pi(n + 1/4)/\omega$. Notice that for the strongly non-Gaussian noise, the first peak is much higher than subsequent ones and its position has a more pronounced deviation from the maximum of the harmonic signal. This indicates that, for this level of additive noise, the threshold crossing is much more likely to occur even in the absence of the periodic input signal on a time scale of the order of the membrane characteristic time constant. Further, the peaks become broader which points to a weaker phase locking and, consequently, reveals an out of resonance condition.

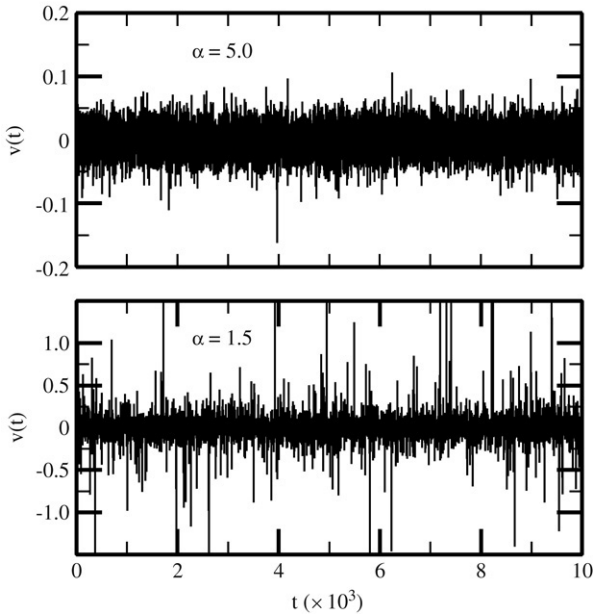

Fig. 2. Typical series generated by the numerical integration of the stochastic differential equation with both additive and multiplicative noises (Eq. (2)) with $\alpha = 5$ (top panel) and $\alpha = 1.5$ (bottom panel). The higher frequency of large events for $\alpha = 1.5$ reflects the strong non-Gaussian character of the noise generated for small values of α.

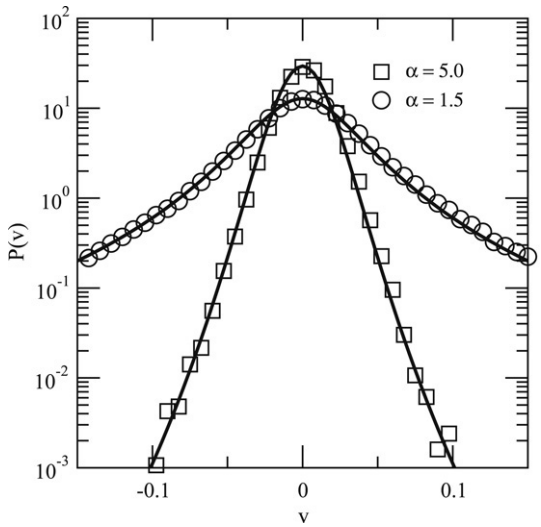

Fig. 3. Distribution function of the two series shown in Fig. 2. The solid lines represent the fits to the theoretical functional form (Eq. (6)) with $\alpha = 5$ (squares) and $\alpha = 1.5$ (circles; $\alpha = (\beta + 1)/2 = (-\lambda/D_\lambda + 1)/2$) and $s^2 = D_\eta/D_\lambda = 1.5 \times 10^{-3}$.

The height of the first-passage-time distribution close to its first three peaks ($t_n = 2\pi(n+1/4)/\omega$, with $n = 0, 1, 2$) is reported in Fig. 5 as a function of the additive noise variance D_η for the same two power-law exponents as are considered above. These curves show clearly the trend typical of stochastic resonance. The peak amplitude goes through a maximum at a specific noise amplitude. The noise amplitudes providing the maxima of each of the peaks are not the same, which is naturally expected because distinct response functions give distinct (although with the same order of magnitude) estimates of the resonance condition [1]. As regards the influence of the noise non-Gaussian character, we can clearly see that the resonance condition is achieved at a much smaller variance of the additive noise for the strongly non-Gaussian noise (one order of magnitude for the cases illustrated). The maximal peak amplitude

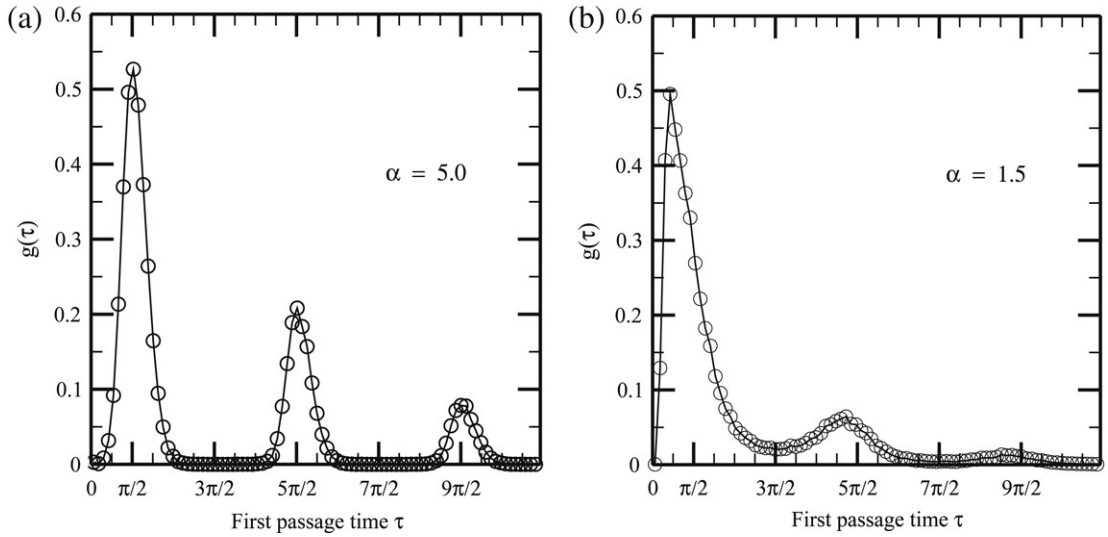

Fig. 4. The first-passage-time distribution as measured from neurons driven by superposed harmonic sub-threshold and noise signals. (a) $\alpha = 5$ and (b) $\alpha = 1.5$. The same levels of additive ($D_\eta = 3.10 \times 10^{-3}$) and multiplicative ($D_\lambda = 1$) noises were considered. The amplitude of the first peak, its displacement from the maximum of the harmonic signal and its broad distribution for the strongly non-Gaussian case shown in (b) indicate that this noise level is quite far above the stochastic resonance condition.

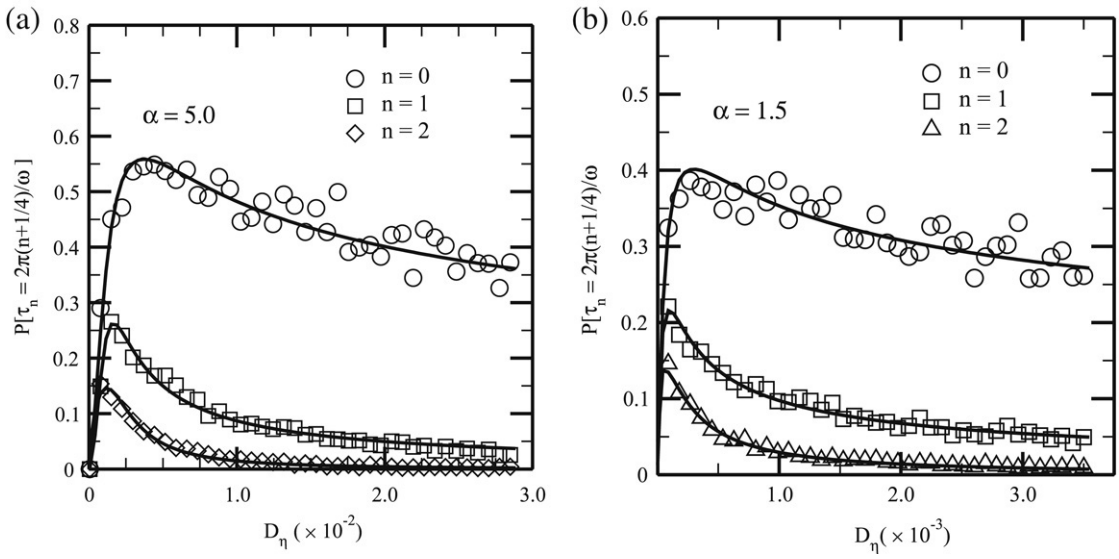

Fig. 5. The amplitude of the first-passage-time distribution at $t_n = 2\pi(n + 1/4)/\omega$ for $n = 0, 1, 2$ as a function of the additive noise strength D_η. (a) $\alpha = 5.0$ and (b) $\alpha = 1.5$ illustrate weakly and strongly non-Gaussian noises. These curves go through a maximum signaling a stochastic resonance phenomenon. The additive noise variance giving the resonance condition decreases as one further deviates from the Gaussian behavior. The noise variance is in units of $D_\lambda = 1$. Solid lines are to guide the eyes.

for the non-Gaussian noise is smaller than that for the Gaussian noise. This feature reflects the fact that the spikes with large noise amplitudes are playing a role in the level crossings. The low frequency of these spikes favors the neuron firing at large times to the detriment of firing at the first maximum of the harmonic sub-threshold input signal.

In Fig. 6 we show that the additive noise variance at which the peaks of the first-passage-time distribution are maximal do indeed decrease continuously with the decay exponent α. However, in order to better characterize the neuron response, it is more appropriate to analyze the resonance condition with regard to the variance of the neuron input noise that results from the random multiplicative process. Actually, the mean square deviation of the input

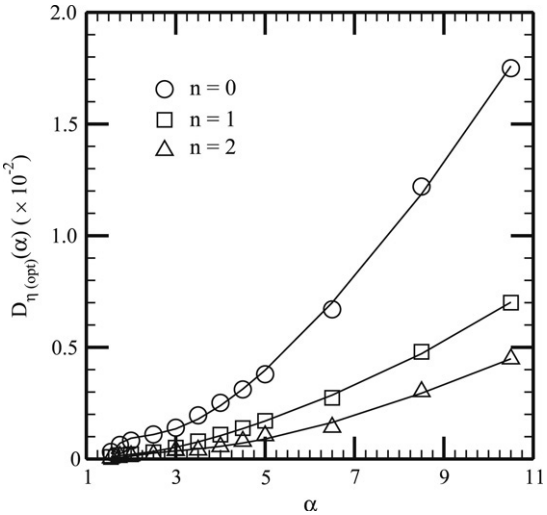

Fig. 6. D_η at the resonance condition versus the decay exponent α of the input noise distribution. The optimal conditions based on the first three peaks of the first-passage-time distribution are shown. The noise variance is in units of $D_\lambda = 1$. Solid lines are to guide the eyes.

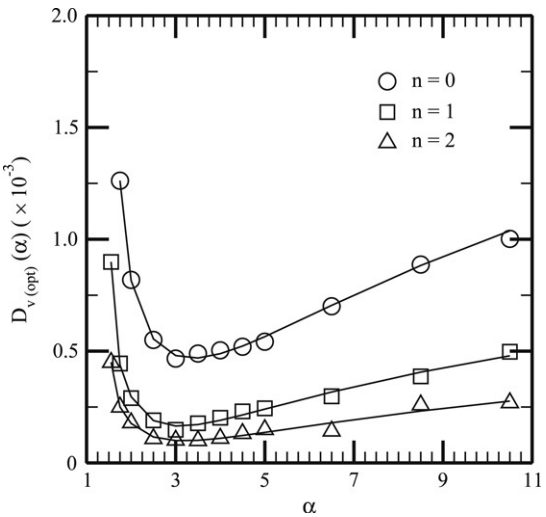

Fig. 7. The optimal input noise variance $D_{v(opt)}$ at the resonance condition versus the decay exponent α of the input noise distribution. The optimal conditions based on the first three peaks of the first-passage-time distribution are shown. The minimum signals the noise distribution providing the most efficient neuron response. The noise variance is in units of $D_\lambda = 1$. Solid lines are to guide the eyes.

noise is divergent for any $\alpha < 1.5$ due to the slowly decaying tail of its probability distribution. Therefore, when reporting the resonance condition with respect to the input noise, as depicted in Fig. 7, one obtains that the optimal input noise variance $D_{v(opt)}$ passes through a minimum at a finite value of the decay exponent. This feature indicates that the neuron ability to identify a sub-threshold periodic signal can be made more efficient, i.e., to require a weaker superposed noise, when the input noise statistics is non-Gaussian with a well defined asymptotic power-law decay. We also analyzed the influence of the stimulus frequency ω on the above result. We found that the power-law decay exponent giving the minimum noise variance at resonance is roughly independent of ω, although the minimum noise level increases for lower frequencies. It is important to stress that the input noise develops a characteristic correlation time as a function of the decay exponent α [42,43]. However, the correlation time remains finite as $\alpha \to 3/2$, thus indicating that the non-Gaussianity of the noise probability distribution is indeed the main ingredient leading to a minimum of the noise variance at resonance.

4. Summary and conclusions

In summary, we have studied the dynamics of the integrate–fire neuron model driven by a sub-threshold harmonic signal. The neuron firings due to level crossings were induced by the presence of a non-Gaussian noise. The input noise was considered as the result of a random multiplicative process displaced from the origin by a small additive noise term. As a consequence, the neuron input noise displays an amplitude distribution with a slowly decaying power-law tail whose characteristic exponent was continuously tuned. By numerically solving the neuron dynamic equation, we computed the first-passage-time distribution which was used as a tool for investigating the stochastic resonance phenomenon occurring in this model, namely, the optimal identification of the sub-threshold periodic stimulus at a finite variance of the input noise. In the first-passage-time distribution, the resonance condition is signaled by its peaks that have maximal heights at intermediate noise intensities. Our main finding was that the neuron input noise variance at the resonance condition reaches a minimum for a finite value of the decay exponent of the noise probability distribution function. This feature reflects the two competing roles played by the non-Gaussian aspect in the noise-induced level crossings. The long tail of the probability distribution favors the occurrence of large noise fluctuations. Although these large fluctuations can promote neuron firings and contribute to the recognition of the sub-threshold signal, its own generation enhances the average noise variance. The ideal balance between these two trends gives the optimal stochastic resonance condition. This mechanism is quite general. Although we have numerically demonstrated its influence on the first-passage-time distribution of the simple integrate and fire model, such competition will produce similar effects on more realistic neuron models which can also be identified by probing other relevant quantities such as the interspike-interval distribution and the signal-to-noise ratio.

It is worth mentioning here that a similar effect has already been identified as regards the presence of power-law correlations in the input noise [14–16] and conjectured to be relevant to the evolutionary adaptation of the biological neural networks. Since non-Gaussian noises are also commonly generated by biological systems [44–47], in particular the internal noise generated by neural networks [48], the results reported here indicate that neural systems may also benefit from the non-Gaussian character of the input noise to enhance the functionality, being able to detect a sub-threshold signal with a smaller noise level than would be required under the influence of a Gaussian noisy environment.

Acknowledgments

This work was partially supported by the Brazilian research agencies CNPq, CAPES and FINEP, as well as by the Alagoas state research agency FAPEAL.

References

[1] L. Gammaitoni, P. Hänggi, P. Jung, F. Marchesoni, Rev. Modern Phys. 70 (1998) 223.
[2] A. Guderian, G. Dechert, K. Zeyer, F. Schneider, J. Phys. Chem. 100 (1996) 4437.
[3] X. Godivier, F. Chapeau-Blondeau, Europhys. Lett. 35 (1996) 473.
[4] D. Petracchi, I.C. Gebeshuber, L.J. DeFelice, A.V. Holden, Chaos Solitons Fractals 11 (2000) 1819.
[5] T. Mori, S. Kai, Phys. Rev. Lett. 88 (2002) 218101.
[6] A. Longtin, J. Statist. Phys. 70 (1993) 309.
[7] E.V. Pankratova, V.N. Belykh, E. Mosekilde, Eur. Phys. J. B 53 (2006) 529.
[8] T. Munakata, M. Kamiyabu, Eur. Phys. J. B 53 (2006) 239.
[9] L. Gammaitoni, E. Menichella-Saetta, S. Santucci, F. Marchesoni, C. Presilla, Phys. Rev. A 40 (1989) 2114.
[10] J. Feng, B. Tirozzi, Phys. Rev. E 61 (2000) 4207.
[11] D. Nozaki, Y. Yamamoto, Phys. Lett. A 243 (1998) 281.
[12] D. Nozaki, J.J. Collins, Y. Yamamoto, Phys. Rev. E 60 (1999) 4637.
[13] A. Bershadskii, E. Dremencov, D. Fukayma, G. Yadid, Europhys. Lett. 58 (2002) 306.
[14] D. Nozaki, D.J. Mar, P. Grigg, J.J. Collins, Phys. Rev. Lett. 82 (1999) 2402.
[15] R. Soma, D. Nozaki, S. Kwak, Y. Yamamoto, Phys. Rev. Lett. 91 (2003) 078101.
[16] Y.G. Yu, R. Romero, T.S. Lee, Phys. Rev. Lett. 94 (2005) 108103.
[17] H.S. Wio, S. Bouzat, Braz. J. Phys. 29 (1999) 136.
[18] M.A. Fuentes, R. Toral, H.S. Wio, Physica A 295 (2001) 114.
[19] M.A. Fuentes, H.S. Wio, R. Toral, Physica A 303 (2002) 91.
[20] F.J. Castro, M.N. Kuperman, M. Fuentes, H.S. Wio, Phys. Rev. E 64 (2001) 051105.
[21] M.A. Fuentes, C.J. Tessone, H.S. Wio, R. Toral, Fluct. Noise Lett. 3 (2003) L365.
[22] J.F.L. Freitas, M.L. Lyra, Int. J. Modern Phys. C 14 (2003) 303.

[23] M.E.J. Newman, Contemp. Phys. 46 (2005) 323.
[24] D. Sornette, R. Cont, J. Phys. I 7 (1997) 431.
[25] D. Sornette, Phys. Rev. E 57 (1998) 4811.
[26] S. Kitada, Physica A 370 (2006) 539.
[27] S. Solomon, P. Richmond, Physica A 299 (2001) 188.
[28] Y. Louzoun, S. Solomon, Physica A 302 (2001) 220.
[29] A.H. Sato, Physica A 344 (2004) 211.
[30] J.L. Cabrera, J. Gorronogoitia, F.J. de la Rubia, Phys. Rev. E 66 (2002) 022101.
[31] A. La Barbera, B. Spagnolo, Physica A 314 (2002) 120.
[32] R. Jain, S. Ramakumar, Physica A 273 (1999) 476.
[33] H. Nakao, Phys. Rev. E 58 (1998) 1591.
[34] A.R. Bulsara, T.C. Elston, C.R. Doering, S.B. Lowen, K. Lindenberg, Phys. Rev. E 53 (1996) 3958.
[35] H.E. Plesser, S. Tanaka, Phys. Lett. A 225 (1997) 228.
[36] T. Shimokawa, K. Pakdaman, T. Takahata, S. Tanabe, S. Sato, Biol. Cybernet. 83 (2000) 327.
[37] T. Verechtchaguina, I.M. Sokolov, L. Schimansky-Geier, Europhys. Lett. 73 (2006) 691.
[38] H.E. Plesser, T. Geisel, Phys. Rev. E 63 (2001) 031916.
[39] A.R. Bulsara, S.B. Lowen, C.D. Rees, Phys. Rev. E 49 (1994) 4989.
[40] T. Shimokawa, A. Rogel, K. Pakdaman, S. Sato, Phys. Rev. E 59 (1999) 3461.
[41] C.W. Gardiner, Handbook of stochastic methods for physics, in: Chemistry and Natural Sciences, Springer-Verlag, Berlin, 1999.
[42] A.H. Sato, H. Takayasu, Y. Sawada, Fractals 8 (2000) 219.
[43] M.P. da Silva, M.L. Lyra, M.V.D Vermelho, Physica A 348 (2005).
[44] M.S. Fee, P.P. Mitra, D. Kleinfeld, J. Neuro. Meth. 69 (1996) 175.
[45] D.C. Bertiloni, D.S. Killen, IEEE J. Ocean. Eng. 26 (2001) 285.
[46] M. Kotulska, S. Koronkiewicz, S. Kalinowski, Phys. Rev. E 69 (2004) 031920.
[47] M.R. DeWeese, A.M. Zador, J. Neurosci. 26 (2006) 12206.
[48] G. Mato, Phys. Rev. E 59 (1999) 3339.